An Investigation of the Materials Science of Metal Vapor Condensate Generated During Selective Laser Melting of Ti6Al4V

Sarah Supatra Waddell

A thesis

submitted in partial fulfillment of the

requirements for the degree of

Master of Science

University of Washington

2023

Committee:

Dwayne Arola

Ramulu Mamidala

Kay Blohowiak

Hsien-Lin Huang

Program Authorized to Offer Degree:

Materials Science and Engineering

University of Washington

Abstract

An Investigation of the Materials Science of Metal Vapor Condensate Generated During Selective Laser Melting of Ti6Al4V

Sarah Supatra Waddell

Chair of the Supervisory Committee:
Dwayne Arola
Department of Materials Science and Engineering

Advancements in metal additive manufacturing (AM) will enable the development of complex components with lower buy to fly ratio, which is highly attractive for aerospace applications. However, one concern in the process of selective laser melting (SLM) of metals is the particulate waste byproducts. The laser-based process produces ejected material (ejecta) and metal vapor condensate (MVC) that must be vented out of the machine. MVC consists of nano-scale particles that are hazardous and require costly disposal methods that are toxic to the environment. Presently, there is limited understanding of MVC produced from SLM and its reactivity.

Here, we explored different techniques to collect and characterize the waste ejecta including MVC produced during SLM with an EOS M 290 printer and Ti6Al4V powder. The ejecta was collected within the printing chamber, on the ventilation exhaust baffle using ex-situ and in-situ methods. Scanning electron microscopy (SEM), dynamic light scattering (DLS) and

Energy dispersive X-ray spectroscopy (EDS) was used for characterization of the MVC. Results showed that the in-situ approach to collection was superior, and that the MVC formed agglomerated networks of individual 20-40 nm particles with a chemical composition of higher Al content in comparison to the feedstock powder. A preliminary analysis of the MVC combustion behavior was performed using bomb calorimetry and thermogravimetric analysis (TGA) to quantify the reactivity behavior and to compare the effectiveness of selected passivation methods. Lastly, samples of ejecta were treated with proprietary chemicals to dissolve the metal byproduct, which was found to be an effective method for eliminating the MVC. The significance of the findings and important next steps are discussed.

Table of Contents

List of Figures

List of Tables

Acknowledgements

I would like to thank Professor Dwayne Arola for his support over the last five years. His endless belief in his students and high standards created an environment that helped the shy student in me become more confident. I would also like to thank Alex Montelione for helping me with all hands-on activities in lab and for being a great mentor, I couldn't ask for better people to work with. This work would not be possible without the contributions of Professor Ramulu Mamidala, Dr. Kay Blohowiak and Hsien-Lin (Stacey) Huang of the Boeing Company, as well as Dr. Marvin Hawkins of Sentecor Solutions. Their technical support and guidance throughout this project were invaluable. This study was also made possible through support from the Joint Center for Aerospace Technology Innovation (JCATI). Lastly, I would like to thank my friends and family for their unconditional love and support.

Chapter 1 - Introduction

1.1 Background of Metal Additive Manufacturing

The use of 3D-printing is increasing rapidly across many industries as an advanced method of manufacturing. Additive manufacturing (AM) or 3D-printing relies on building a part layer-by-layer directly from a computer aided design, rather than subtracting material from a billet or injecting material into a mold. There are a number of advantages of AM in comparison to competing traditional methods of manufacturing, but one of the most beneficial is the minimum buy to fly ratio for finished parts. As such, AM processes are extremely attractive for the aerospace industry.

Focusing on the applications in aerospace, there has been great interest in the advantages of metal AM over traditional manufacturing methods. Because parts can have more complexity with AM, designs can be optimized for weight reduction, thermal performance, and mechanical durability with less concern for the manufacturability [1]. The flexibility of AM also allows parts to be combined in one print and reduce the need for fastening pieces together, ultimately improving the system performance and reducing the number of components overall. 3D-printing can also be performed “on-demand”, which can result in a substantial reduction in lead-time.

Powder bed fusion (PBF) has become one of the most prevalent types of metal AM processes in industrial settings [2]. This involves depositing a thin layer of metal powder and using a power source to sinter or melt the powder together in layers as shown in **Fig. 1**. Powder is spread across the printing bed and the power source will fuse the required layer; then the bed will move lower in increments to make room for the next layer of powder to be spread on top. PBF by melting has become more prevalent over sintering as melting leads to higher part density

[2]. The power source used tends to either be a laser, e.g., in selective laser melting (SLM), or an electron beam used in electron beam melting (EBM).

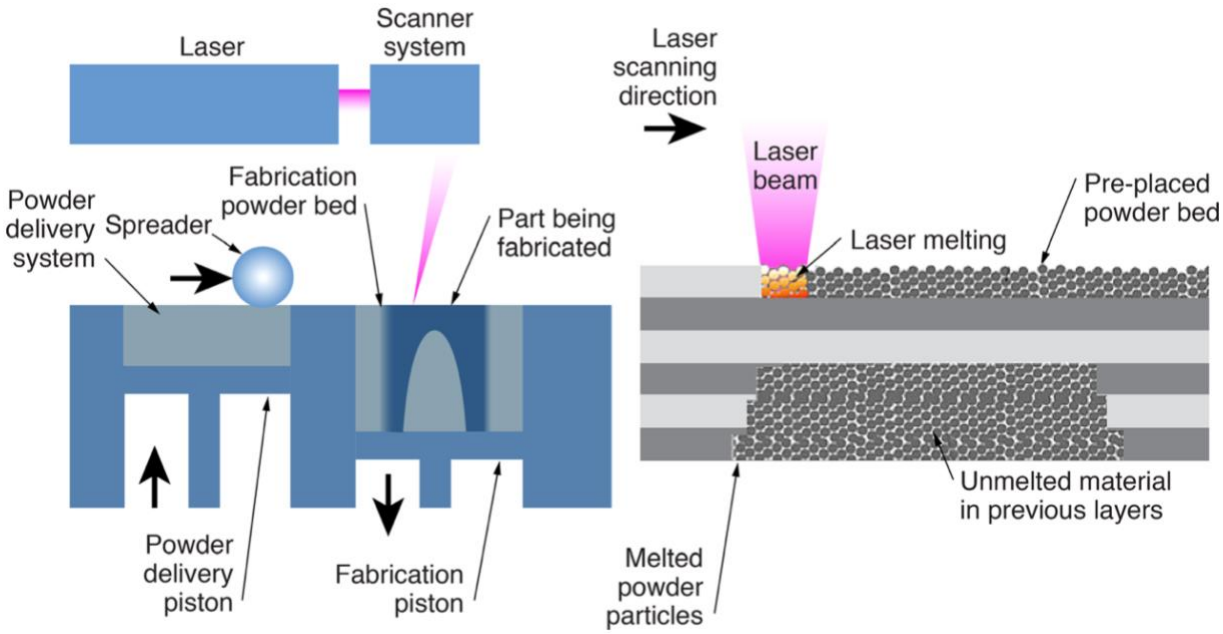

Figure 1. The SLM printing process, with the left side showing the powder distribution system and the right side showing the laser melting process of each powder layer. Reproduced from [1].

The primary focus in PBF technologies is increasing the cost effectiveness of both the machines and powder feedstock, as well as maximizing the metal quality, mechanical properties and the performance of printed parts. An important issue that has received limited attention involves the byproducts that are generated and how they are dealt with. For instance, in SLM hazardous nano-scale waste metal is created through interaction between the laser beam and powder. Unlike EBM which occurs in vacuum, SLM requires that the byproduct materials generated during a build are vented out of the chamber through a filtration system and into a container. These byproducts have been a growing concern [3, 4]. And as the use of metal AM

becomes more prevalent in the aerospace industry, there is greater need for understanding these hazardous materials and how to best dispose of them.

1.2 The Phenomenon of Particulate Waste Metal

It is necessary to describe how fine metal byproducts are produced in SLM. As the laser scans and heats the feedstock powder, a melt pool is created which undergoes intense super-heating. The high thermal energy density associated with the heating process causes vaporization of metal and the ejection of heat-affected powder, which is commonly termed *ejecta* [3]. This phenomenon is similar to the metal plumes that occur from welding [5]. **Fig. 2A** shows a schematic of the melt pool caused by the laser within SLM. Rapid vaporization of metal can cause instabilities within the melted region and cause ejection of melted material, known as *spatter*, alongside with the *ejected powder* [6]. Spatter tends to have a large range of sizes, mainly being larger than the original feedstock powder, which usually has a diameter of around 20-80 μm in SLM. The vaporized metal undergoes rapid cooling in the build chamber and solidifies into nanoparticles, referred to as *metal vapor condensate* (MVC). An accumulation of MVC in the build chamber can cause attenuation of the laser and lead to poor metal/part quality due to a lack of beam focus [6, 7].

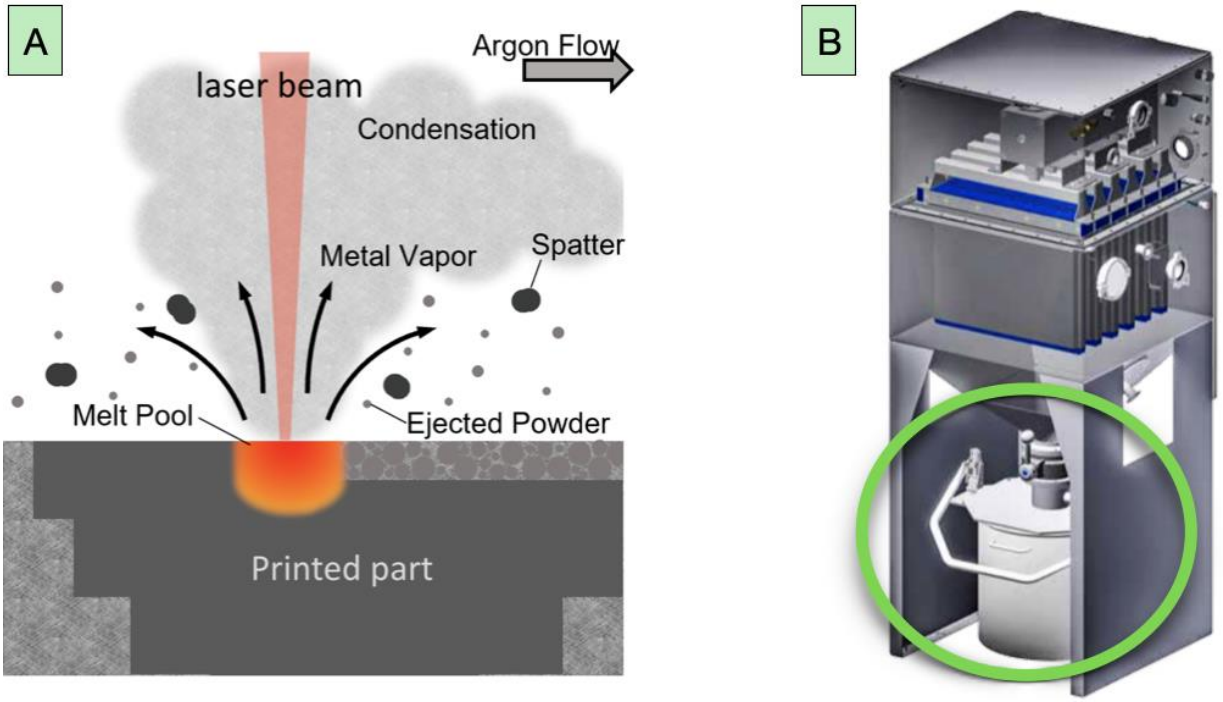

Figure 2. Details of byproducts generated in SLM. (**A**) a diagram depicting the production of ejecta from the melt pool during SLM printing, and (**B**) a waste collection system for metal AM by Herding Filtration Systems; the waste container is circled in green [8].

To overcome problems associated with the MVC and other potential reactions between the molten metal and build environment, an inert gas stream such as argon is constantly swept over the print bed surface, carrying the ejecta through an exit vent and into a waste container as depicted in **Fig. 2B**. However, many researchers have found ejecta remaining within the printing chamber [6]. Sutton et al. collected spatter from the printing-chamber walls, and further suggested that an accumulation of ejecta could be one of the factors compromising powder reuse.

There has been significant effort to reuse printing powder to reduce waste and cost, but feedstock powder undergoes a degradation after being reused many times [9]. Santecchia et al. commented that parts built with reused powders exhibit much more variation and less predictable

mechanical properties. They emphasized that the gas flow must be tuned to effectively remove as much of the byproducts as possible [3, 10].

1.3 Survey of Metal Vapor Condensate (MVC)

There have been limited studies reported in the open literature that focus on MVC and characterize the size, morphology and other aspects of particulate [7, 11, 12]. Two different studies that involved printing stainless steel and titanium powders reported that MVC tends to arrange in agglomerations of nanoparticles on the scale of tens of nanometers [6, 7, 12]. Sutton et al. identified MVC adhered to most surfaces of the build chamber and was near black in color [6]. Keaveny et al. studied MVC produced from Ti6Al4V during SLM and found that the individual size range of the nanoparticles were typically 10 to 20 nm from SEM images [7]. In that study, samples of MVC were collected by wiping the build chamber wall with a lens cleaning swab, and then rinsing the powder off with alcohol. The smaller particles became suspended in the alcohol and were pipetted onto sample holders for electron imaging methods. Of significance, Keaveny et al. found that MVC had a higher concentration of Al and a lower concentration of Ti in comparison to the feedstock powder. Noskov et al. found aggregated ultrafine particles with diameters of 4-16 nm produced from stainless steel laser-based printing. In that effort the mVC was collected by placing air filtration cassettes in the build chamber to collect material during printing [12].

Other relevant studies of MVC studies involve measuring levels of MVC in the air as a respiratory risk. Of concern, MVC particles have been found to be released during certain activities apart from printing, such as when emptying and cleaning the print chamber [13, 14]. Jensen at al. collected particles released from the machine on copper mesh and found that the

majority of particles were under 200 nm, withan average size being between 53 and 70 nm [13]. Nano-sized TiO2 may cause genetic damage and aluminum has shown to be a neurotoxin. Therefore, it is critical to use proper protective equipment when dealing with large quantities of used printing powder or ejecta. Clearly, this topic is of significant importance to the future of SLM and its industrialization. Nevertheless, this topic has been largely overlooked.

Despite the importance of vaporized metal byproducts in SLM to printing and part quality, as well as the tremendous safety concerns, research performed in this area is limited. One of the critical limitations is acquiring the MVC for scientific examinations. While spatter can be filtered out of the feedstock as a part of the powder recovery process, the fine particles of MVC mainly end up in a waste container, similar to the one depicted in Fig. 2B. Nano-scale dust is at risk of combustion, especially when containing metals that rapidly oxidize like titanium or aluminum [4, 15]. Of note, there have been incidents of large metal dust explosions in factories that focus on metal products, and metal AM sites storing large quantities of condensate waste has been a source of concern [4]. Therefore, the waste container must be properly passivated in accordance with EPA requirements [16]. The most common approach is to use an oil and sand for containment. Silicone oil is preferred over mineral oil to inhibit the flash reaction, and flocculants are often recommended such as chalk or quartz sand to disperse the metal particles. The treated waste is then transported to a specialized waste site and often disposed or incinerated [16]. Handling of the waste is hazardous and costly. With the momentum towards adoption of metal AM in aerospace and the projected high volumes of production, the treatment of metal waste byproducts can create a significant cost to organizations operating SLM printers.

1.4 Metal Nanoparticle Reactivity

Much of the previous research involving MVC has been focused on understanding its threat to printing conditions or respiratory health. Surprisingly, no reported efforts were found on the combustion hazard. While the reactivity of MVC in metal AM has not been discussed in the open literature, there has been extensive research into the combustion of metal nanoparticles for applications such as explosives and solid fuel [17]. There are many advanced techniques for analyzing nano powder combustion including flame burners or shock tubes equipped with high-speed cameras to measure burn times [17, 18-20]. But these methods either require significant quantities of over a gram of material, or they were not available for access to the UW group.

The two most accessible methods for measuring reactivity that require relatively small amounts of material were bomb calorimetry [21] and thermogravimetric analysis (TGA) [22-25]. Tran et al. demonstrated using bomb calorimetry to analyze the combustion of aluminum powder of 15 μm and 160 μm [21]. They placed 35 to 50 mg of powder in a packing peanut to disperse the powder more evenly than mixed in a solution. This is a large amount of powder when it comes to collecting MVC, and it would likely be difficult to get a high enough resolution from samples of closer to 1 mg of metal powder. TGA on the other hand requires a much smaller sample mass. Noor et al. conducted TGA-DSC of aluminum nano particles with sample quantities of 6 mg at different heating rates and found that ignition occurred at ramp rates equal to or above 8 K/min [22]. Ideally, this technique could be used to observe ignition of MVC from changing temperature ramp rates.

Here, we conducted investigations involving bomb calorimetry to connect the process of ejecta collection to characterizing the reactivity of collected material. These two components go hand-in-hand as the method of collection controls the volume of acquired MVC, which then contributes to the reliability of the methods of characterization. We hope to lay a foundation for

future efforts focused on evaluating the byproducts of metal AM, which will ultimately support the development of improved methods for safely handling and disposing of MVC.

1.5 Objectives

This project was motivated by the limited understanding of the nano-particle waste produced from SLM printers across both industry and in the literature. Condensed metal vapor is known to be dangerous in large quantities, but there are currently no studies quantifying the reactivity of MVC and/or the effectiveness of different methods of passivation. One of the primary concerns is the limited understanding of the MVC itself; a thorough characterization of MVC for SLM of Ti6Al4V, a predominant metal in the aerospace industry, does not exist. This project intended to identify plausible approaches to collect, characterize and potentially eliminate MVC generated in printing Ti6Al4V by SLM.

The specific aims of this project include:

i) Develop methods for collecting MVC generated in SLM that are safe and that will support advanced characterization of the material
ii) Identify methods that enable robust characterization of the MVC and develop further understanding of the material composition and morphology
iii) Evaluate potential methods of digesting or passivating MVC, and identify test methods to characterize their effectiveness

Past investigations of MVC have relied on hanging sample collectors or sampled material from the chamber walls [7, 12]. In this project, we explored various collection methods

to find the best approach to collection that would enable reactivity experiments. One of the main challenges to collecting MVC was that we were unable to access the MVC waste container (Fig. 2). Dealing with metal nanoparticles in large quantities poses a severe health risk. Consequently, the team pursued the collection of small volumes of material from within the build chamber and accessible through the chamber door. We used an ex-situ method of swabbing ejecta from the inside of the chamber and compared this method to an in-situ approach of leaving collection tabs in the chamber exit gas flow during printing. We found that the in-situ method involving the placement of collection tabs at strategic ventilation points inside the printing chamber collected significant quantities of MVC, with respect to the ex-situ approach. These amounts were enough to characterize the morphology and chemistry, as well as the reactivity.

Chapter 2 - Materials and Methods

2.1 Printer and Materials

The metal printer used for producing MVC was the EOS M 290 (EOS GmbH, Germany), located at the University of Washington. That system is operated with a 400 W Yb-fiber laser and spot size of around 80 μm. Printing with this machine is performed exclusively with Grade 5 Ti6Al4V powder. The printing bed is 250 x 250 mm with a build height of 350 mm. All prints or builds for this project were conducted with an inert argon atmosphere. The machines were cleaned thoroughly in between each print with a wet-separator vacuum. This process does not fully remove the material built up in areas such as the exit gas vent.

The EOS M 290 uses a fiberglass paper filter in the filtration system (EOS H13 Particle Filter), which was also used for collection methods. Other materials used for collection involved

carbon SEM tape, copper foil SEM tape, and nylon membrane disc filters (0.22 μm, Southern Labware, Georgia). Tabs used for in-situ collection included stainless steel paper clips with a 0.8 by 1.2 cm rectangle of collection material of either fiberglass or carbon tape.

For reactivity measurements a 99.9% titanium nano powder (US Research Nanomaterials, Inc, Texas) was used as a commercially available nanoscale material that was more standardized than MVC. The titanium nano powder was spherical with a 70 nm diameter and produced form electrical explosion method.

2.2 Characterization Instruments

Particle size analysis was conducted using dynamic light scattering (DLS) and scanning electron microscopy (SEM). DLS was used to measure the range of fine particle sizes found below the size scale of spatter (effective diameters $\leq$ 20 μm), whereas SEM was used to measure individual nanoparticles. The DLS evaluations were performed using a Malvern Zetasizer Nano ZS (Malvern Panalytical Ltd, United Kingdom), which has the capability of measuring between 0.3 nm to 10 μm. The refractive index used was set to 2.7 based on the standard value for titanium. Either deionized (DI) water or ethanol were used as the main solution to suspend the metal particles, which were sonicated for 10 minutes before pipetting the sample out.

Two different types of SEM instruments located at the University of Washington were used for evaluation of the MVC, including a TFS Apreo 2 variable-pressure SEM (Thermo Fisher Scientific, Massachusetts) and a Sirion XL30 SEM (FEI, Oregon). Scanning electron microscopes were useful for observing the presence of MVC within samples containing larger particles. To measure individual nanoparticle sizes, ImageJ (Version 1.53v, public domain

software by Wayne Rasband) was used on images of 50,000-80,000x magnification at accelerating voltages of 2-5kV. Both of the SEM instruments included an energy dispersive X-ray spectroscopy (EDS) detector for elemental analysis. The working distance used for EDS was set at about 10 mm, whereas a distance of 3-5 mm was used for taking images.

Thermal analysis of the MVC was performed using bomb calorimetry and thermogravimetric analysis (TGA). A 1341 Plain Jacket Bomb Calorimeter (Parr Instrument Company, Illinois) was accessed on the UW campus. The bomb was pressurized with 25 atm of oxygen and placed in 2000 g of water that is constantly being stirred and monitored in temperature. Samples were ignited with 10 cm tungsten fuse wire. The samples tested were ethanol and titanium nano powder, which ranged from 1-2 g in bomb calorimetry. TGA was conducted with a Mettler Toledo TGA/DSC 3+. The sample pans were aluminum oxide crucibles with an inner diameter of 4 mm. An air gas flow of 50 mL/min was used. The mass of samples for TGA ranged from 1-3 mg. Different ramp rates between 5 to 20 °C/min were used, with tests starting at 25 °C and ending at a maximum temperature between 1200-1400 °C.

2.3 Ejecta Collection Methods

This section will provide a description of the various methods used for collecting ejecta from the EOS M290. Although the EOS SLM machine at the UW was not operated frequently, the inner chamber of the EOS machine had a thin layer of dust that provided a useful initial source of ejecta.

2.3.1 Printer Collection Region

All collection of ejecta was performed in the build chamber, with a focus on the exit ventilation structure that is regarded as the baffle as shown in **Fig. 3**. The multiple openings of the baffle face the argon gas source flow, which originates from the nozzles and across the build layer as positioned in **Fig. 4**. Each opening of the baffle is separated by vanes that are slanted to guide the argon gas flow out of the printer and into the filter system. Because most of the vaporized metal is vented out through the baffle, this was a strategic point of sampling to reach the highest concentration of MVC. The vanes are labeled 0-5, with vane 0 being closest to the chamber exit or proximal end, and vane 5 being the furthest at the distal end.

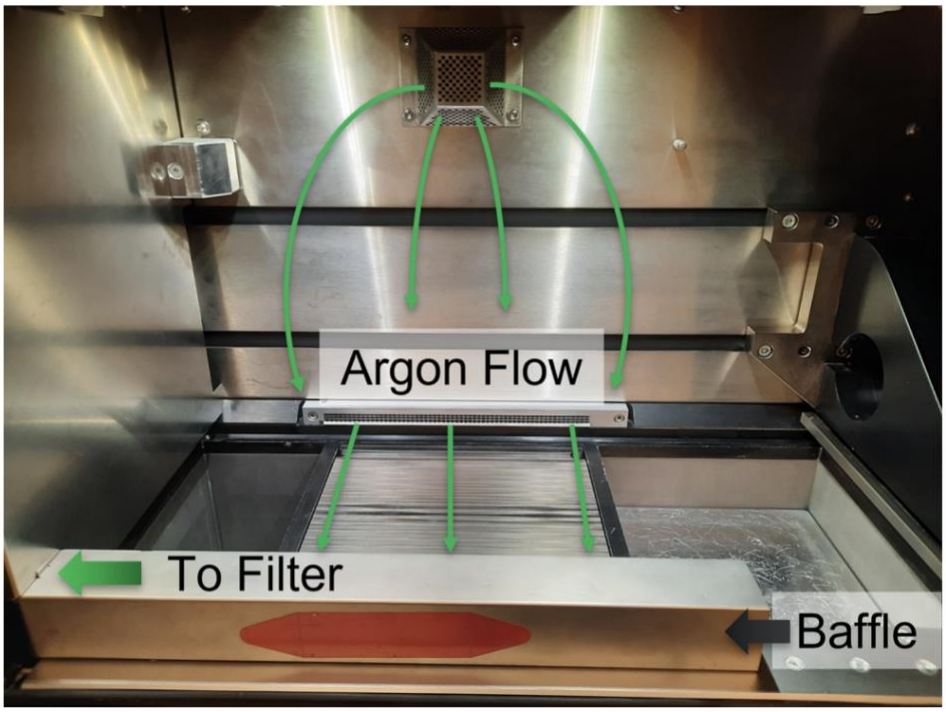

Figure 3. The printing chamber of an EOS M 290 depicting the argon gas stream flow across the build plate and into the exit baffle. The gas flow continues within the baffle to the filter system.

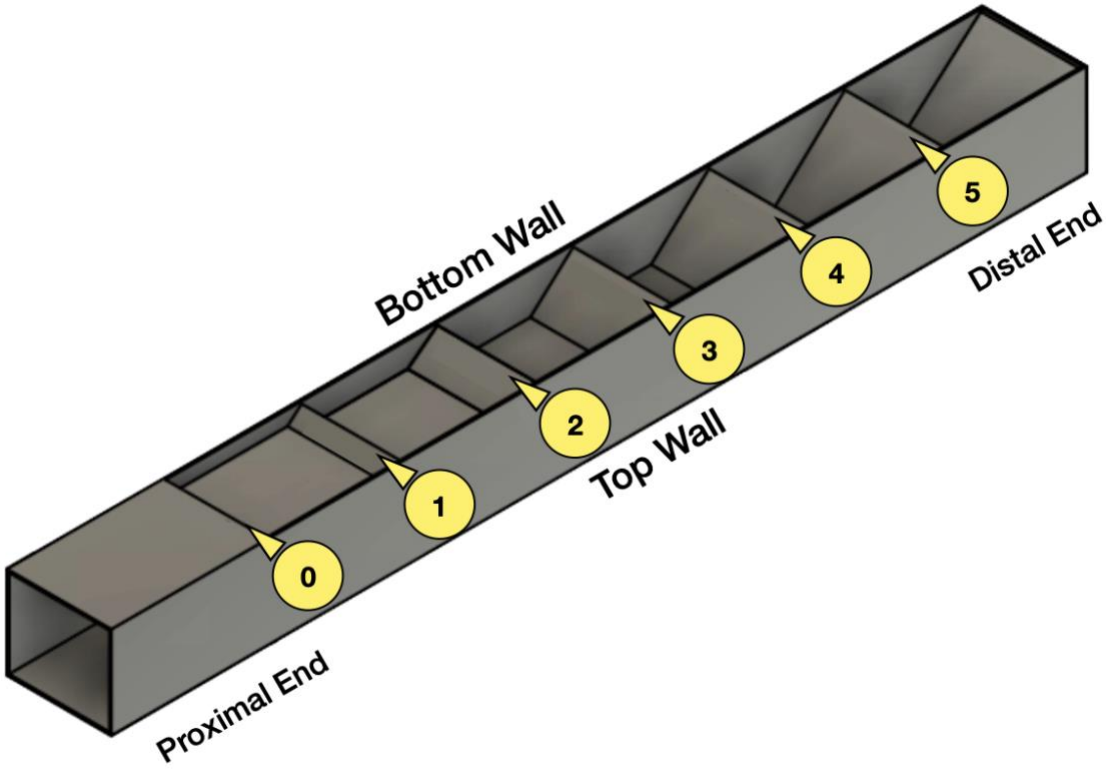

Figure 4. The exit baffle for delivery of the argon gas exhaust. The baffle in this schematic is rotated 90° counterclockwise about its longitudinal axis from its position in the build chamber (Figure 3). This orientation reveals the distribution of vanes.

2.3.2 Ex-Situ Sampling Approaches

2.3.2.1 Swabbing the Baffle

Swabbing the baffle was the first approach that was pursued for collection. This technique involved opening the printer after a build and collecting the ejecta that was stuck to the baffle. To collect ejecta, a wet swabbing method was used with filter paper made of either fiberglass or nylon. The original intention was to collect media and conduct passivation or digestion studies directly on the same fiberglass filters used in the SLM printers. Preliminary

results showed that the fiberglass paper was delicate and broke apart easily, whereas the nylon filter swabs performed much better. Briefly, in the swabbing process the filter papers were held with tweezers, soaked in a solution, then swept across the inner baffle sections until the filter paper darkened with metal dust. Ethanol, acetone, methanol and water were all tested as solutions for pre-treatment of the filters. While there was no significant difference in the effectiveness between each solution, ethanol was eventually chosen as the preferred solution as it wicked up dust effectively without evaporating as rapidly as acetone.

When sampling from the baffle, it was found that there were limitations to the swabbing approach with fiberglass and nylon filter tabs. As such, alternative collection methods were pursued to gain insight from a variety of characterization tools. While the fibrous materials enabled a high volume of material to be collected, it was difficult to observe the collected materials at high magnification under SEM or collect elemental data with EDS. This difficulty was not unexpected as the fiberglass and nylon are not conductive under high voltages of over 10kV. To overcome this problem and obtain samples with electrically conductive foundation, portions of carbon tape were pressed against the baffle wall to collect ejecta and related material. It was possible to observe these samples directly using SEM.

2.3.2.2 Collection in Solution

Rinsing the baffle in small doses was also performed to collect ejecta for DLS, which requires suspending particles in solution. First the particles on the baffle surface were agitated with a portion of wet filter paper. Then the baffle was tipped and either water or ethanol was pipetted across the surface and dripped into a collection jar. In order to remove the influence of

large spatter particles, the solutions were sonicated for at least 10 minutes and then the upper portion of the liquid was pipetted out [7, 22].

A substantial degree of effort was expended in isolating the ejecta by pipetting small amounts of the suspension onto copper tape to have a conductive background of desirable chemistry for EDS. Copper is ideal for imaging by SEM and EDS as it is both highly conductive and can be easily removed when assessing elemental composition. The isolation of ejecta was attempted by pipetting the top of the solution containing ejecta in ethanol and centrifuging so that the fine suspended particles became visibly separated. The volume of isolated material, which consisted of no more than a speck, was pipetted out onto a copper surface. This method proved to be unreliable due to the limited visibility of nano-scale metals and high amounts of residue carried over from the solution.

2.3.3 In-Situ Collection

The second principal method for collecting ejecta consisted of attaching sample filter tabs onto the EOS M 290 baffle prior to performing prints with the EOS M290. Each build consisted of a print that consumed around 275 g of Ti6Al4V powder. These prints reached a height of approximately 25 mm and required approximately 12.5 hours to print. This in-situ approach to collection was pursued to obtain a higher concentration of MVC and to obtain a better representative sampling of the ejecta that is vented out of the build chamber rather than is deposited on either the chamber walls or baffle vanes.

To maintain placement of the in-situ filter tabs on the baffle vanes, stainless steel clips were clamped on to the vanes or walls of the baffle. The arrangement used for the first build is shown in **Fig. 5**. In the first trial, filter tabs were placed on almost every possible location,

including on a vane facing the build plate (outer vane), on a vane shielded from the build plate (inner vane), and on the baffle walls at the top and bottom. Of the 18 total samples, 5 were carbon tape for immediate viewing under the microscope and are indicated with a star in Fig. 5.

The tabs placed in the inner vane position appeared to collect more dark metal material, indicative of a higher concentration of MVC. Thus, for the second build, 11 filter tabs were placed on the inner vanes only. We also experimented with adding copper tape to some of the clips in a separate build and found that they still collected some ejecta.

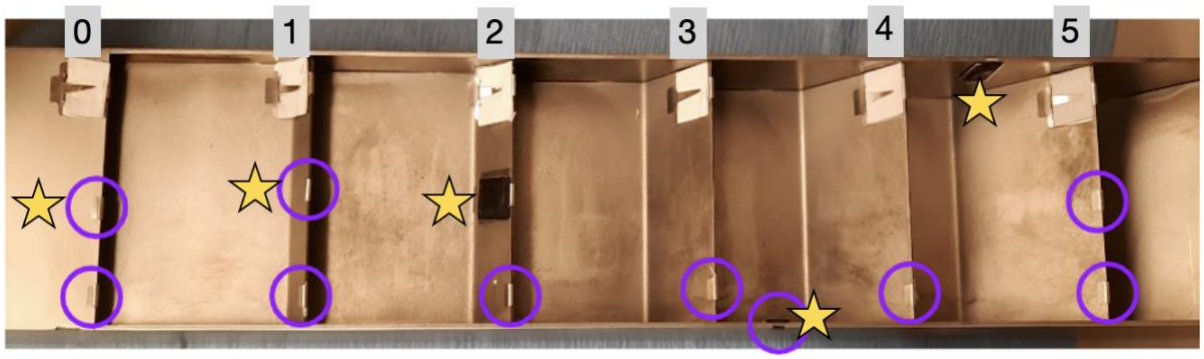

Figure 5. View of the baffle with in-situ collection samples for the first build performed for collecting MVC. Inner-facing tabs are circled in purple and the remainder are outer tabs that face the build plate. All carbon tape samples are noted with stars.

To evaluate the amount of material collected during this in-situ approach, the weight of the filter tabs was recorded before and after each build. A precision balance (Mettler Toledo XPE206 Delta Range, Switzerland) was used, which had an accuracy of 0.005 mg.

2.3.4 Digestion studies

Preliminary studies were performed to evaluate the potential for digestion of the byproducts produced during SLM of Ti6AlV. This effort was conducted in collaboration with

Sentecor Solutions, LLC. Sentecor was an important partner in this program and proposed their proprietary chemicals for digestion of titanium-based metal particles as an alternative to passivation methods. The benefit of dissolving the MVC in solution over passivation was that the disposal steps would be substantially reduced. Three proprietary solutions named Solutions 7, 11 and 12 were used. The pilot studies involved evaluating if ejecta could be removed from their filter as assessed by visual changes as no combustion analysis techniques were available at the time of this effort.

In the first study, the test samples consisted of ejecta on fiberglass filter papers collected from the ex-situ swabbing method. Three different filter samples were observed over a period of 4 hours. A single sample was placed in one of the two chemicals according to the following plan: i) solution 11 at room temperature (20°C); ii) solution 12 at room temperature (20°C); iii) solution 11 at elevated temperature (50°C).

For the second digestion trial, a set of nylon ex-situ samples were used instead of fiberglass. Preliminary studies showed that the nylon didn't fall apart as easily as fiberglass and could be transported with less risk of damage. Three different rinse methods were compared, including: i) 1mL of DI water only, ii) 1mL of solution and 1mL of DI water, and iii) lastly 3mL of solution and 1mL of DI water. The samples were rinsed with the same solution number that they were soaked in. Condition (i) served as the control. The rinse was performed by slowly dripping liquid over the filter sample to reduce any disturbance to the material. Samples in these three conditions were also compared over three different time periods of soaking: 20 minutes, 3 hours, and 24 hours. Three different solutions were also compared. This led to a total sample count of 27 for the three rinse types, three time periods and three solutions as outlined in **Table**

1. Because mass change was not a reliable way of indicating loss of material, macroscopic and microscopic observation of the samples was performed.

Table 1. Experiment conditions for Digestion Study 2

Solutions (#)	7	11	12
Times	20 min	3 hours	24 hours
Rinse Method	(i) 1mL DI only	(ii) 1mL solution, 1mL DI	(iii) 3mL solution, 1mL DI

Chapter 3 - Results

3.1 Evaluation of In-Situ Ejecta Collection

Representative images of a fiberglass tab placed in-situ before and after a print is shown in **Fig. 6A**. This tab was an example of how the tabs at the inner vane position collected material that was very dark, which is believed to indicate a higher ratio of MVC content. Tabs on the outer vane collected material that was lighter in color, as shown in **Fig. 6B** indicating two outer vane samples after Build 1. These tabs facing the build plate likely had significantly more spatter and ejected particles because there was nothing that shielded the samples from the direct stream of material. It was desired to collect MVC without ejecta.

A histogram of the collected weight distribution in the tabs as a function of location along the baffle is shown in **Fig. 6C**. As evident in this figure, the weight of collected ejecta tended to be higher towards the middle of the baffle at Vanes 1 and 2. This may be due to the gas stream directed towards this region as well as the location of parts being printed on the bed plate.

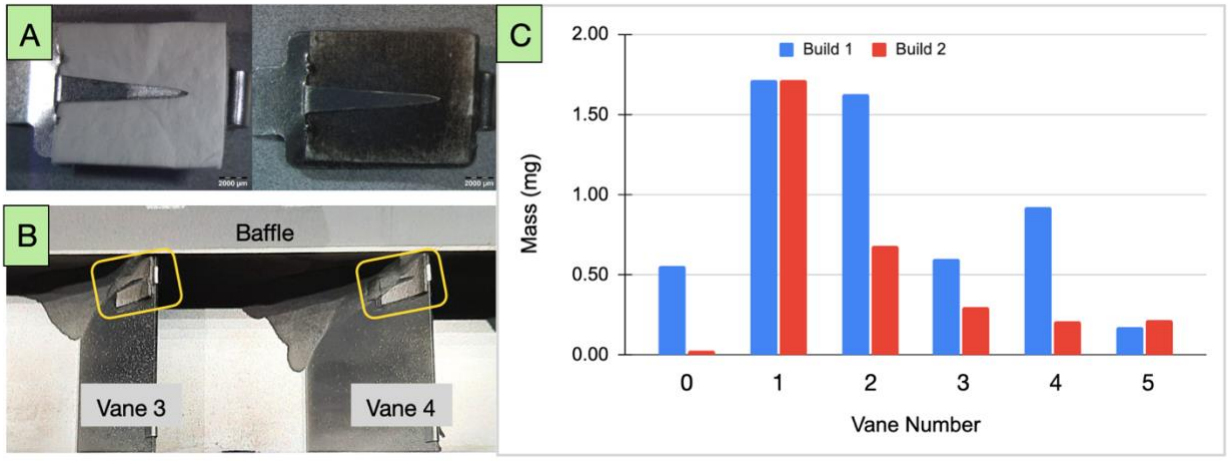

Figure 6. Details of collection. (**A**) an in-situ, inner vane fiberglass filter tab before and after conducting Build 1, (**B**) in-situ filter tabs clipped to the baffle after the print ended, and (**C**) a plot of the net mass increases across the different vanes.

*Note: during Build 1, the collection tab on Vane 0 was dislodged during printing and was found later when cleaning the chamber.

3.2 Characterization of Ejecta

The collected ejecta samples were assessed in different ways to characterize the size, morphology, and chemical composition of the particles and material overall.

3.2.1 Size and Morphology

The MVC particles were identified as individual nanoparticles grouped together in agglomerations as seen in the SEM images of ejecta on carbon tape in **Fig. 7A** and **7B**. The diameters of individual particle were measured as shown in red in Fig. 7A from the in-situ samples collected from each vane of the baffle. A histogram of measurements from three different vanes is shown in **Fig. 8A**. As evident from this distribution, the majority of individual nanoparticles possessed a diameter ranging from 20-40 nm. It was found that there was no dependence of nanoparticle size on collection location as evident from **Fig. 8B**.

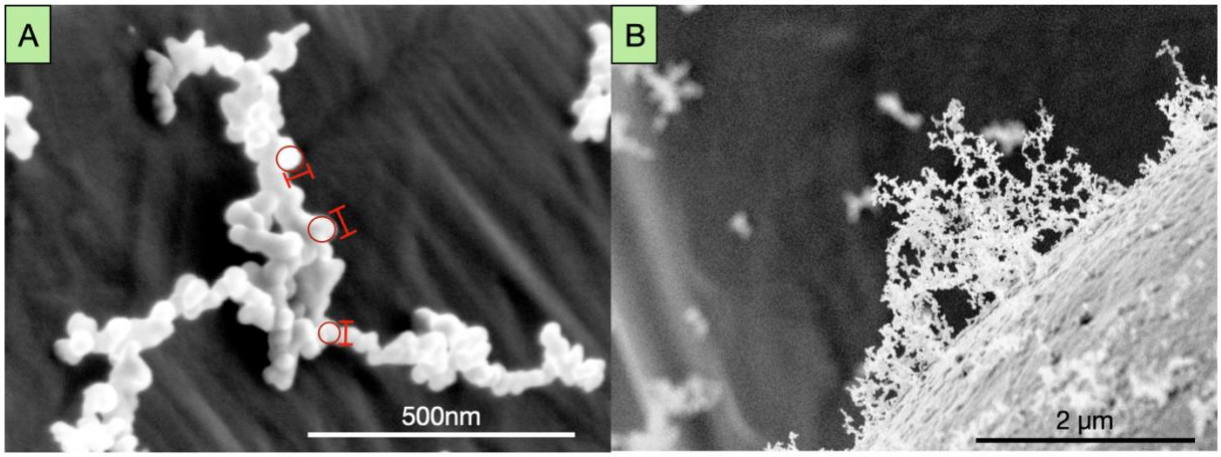

Figure 7. Size and morphology of the MVC. (**A**) SEM image of Ti6Al4V MVC agglomerate indicating how individual nanoparticles were measured with ImageJ, and (**B**) showing larger agglomerations.

*Note: both images were taken on carbon tape, and the MVC were found attached to larger ejecta particles.

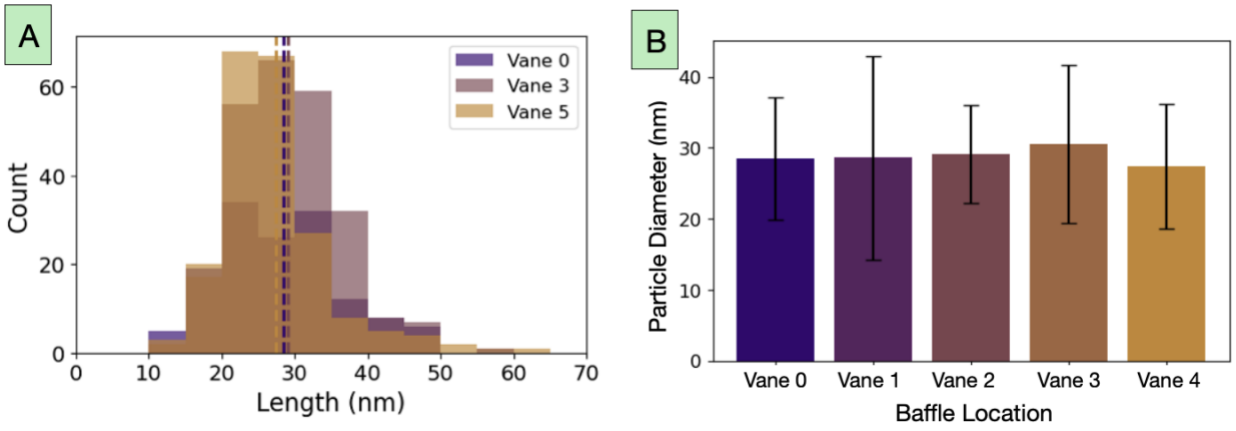

Figure 8. Diameter measurements of the individual MVC particles. (**A**) histogram of the nanoparticle sizes found on three different vanes of the baffle, (**B**) the average nanoparticle size compared across multiple vanes from Build 1.

Fig. 9A shows the sizes of particles collected by ex-situ rinsing and measurement by DLS. Note that this measurement contains particles suspended in solution and excludes larger particles that

sink to the bottom. It is also important to note that the particle size range measured with DLS is different due to the agglomerating nature of the particles. Based on the DLS measurements there are three main size groups, with effective diameters of approximately 200 nm, 900 nm, and roughly 6 μm. The large group in terms of representation is the group with 900 nm diameter. As confirmed by the SEM analysis, these three sizes are likely large agglomerations and small particles ejected from the melt pool, similar to that shown in **Fig. 9B**.

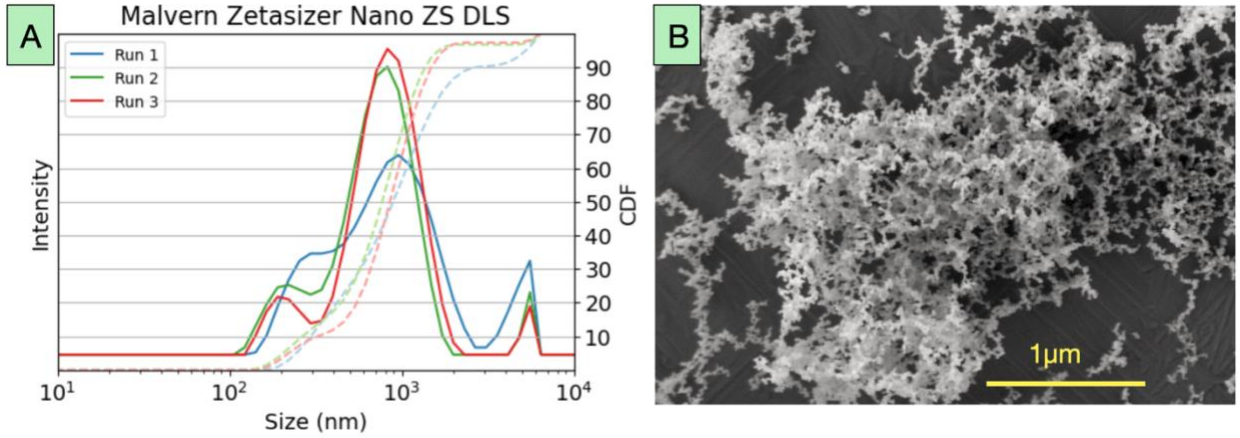

Figure 9. DLS measurement of material from the vanes collected in solution. (**A**) Size distribution from DLS of rinsed and suspended ejecta, (**B**) large mat of Ti6Al4V MVC on an ejected particle.

3.2.2 Elemental Composition

An elemental analysis was performed using EDS on ejecta on both ejected particles and MVC. Because the diameter of the electron beam probe is around 1 μm, large cloud-like groupings of MVC were needed to get reliable elemental data, similar to the mat of MVC shown in **Fig 9B**.

In comparison to the powder feedstock, the MVC was found to have a different chemical composition, as shown in **Table 2**. Specifically, the MVC exhibited higher

concentrations of aluminum, and lower amounts of titanium relative to the original feedstock powder. The difference in chemistry has been attributed to aluminum being much lighter than titanium, and therefore vaporizing more readily in the formation of MVC [7].

Table 2. EDS elemental analysis in wt% of Ti6Al4V ejecta and MVC

Material	Titanium	Aluminum	Vanadium	Oxygen	Carbon
Feedstock Powder	89.27	6.32	4.02	0.15	0.01
Ti6Al4V Ejecta	86.6 ± 1.7	4.3 ± 0.2	3.8 ± 0.1	3.9 ± 0.1	1.4 ± 0.1
Ti6Al4V MVC	79.6 ± 1.8	18.3 ± 1.2	2.0 ± 2.6	—	—

3.3 Digestion Studies

3.3.1 Digestion Study 1

Ejecta samples collected in-situ from Build 1 were soaked in Solutions 11 and 12. We monitored these fiberglass samples visually for signs of the Ti6Al4V ejecta being dissolved. **Fig. 10** shows ejecta samples after times of 5 minutes and 2 hours; the samples lightened in color drastically from the original darkened state. The sample in Solution 12 appeared to lighten faster than the filter swab in Solution 11. Furthermore, the sample soaked in Solution 11 at 50°C appeared to lighten in color faster than at room temperature (20°C) as expected.

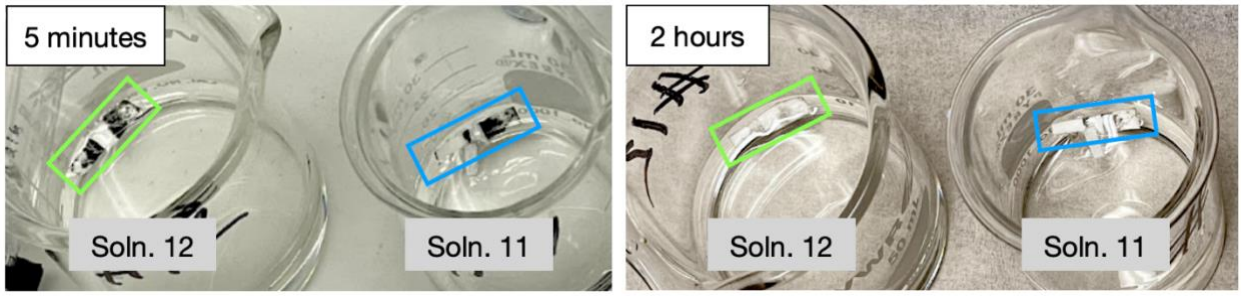

Figure 10. Ex-situ samples placed in Sentecor Solutions 12 and 11 after 5 minutes (left) and after 2 hours (right) at room temperature showing a decrease in ejecta as evident from the color.

An SEM analysis was performed on the treated samples to observe the effects of the solutions and period of exposure. **Fig. 11A** shows the fiberglass sample with ejecta prior to treatment; there is a substantial amount of MVC covering the glass fibers and larger ejected particles. After the samples were soaked in Solution 11 at room temperature, the fibers were covered in residue left from the solution as seen in **Fig. 11B**. Weight measurements revealed that there was never more than a 0.05 mg decrease in weight. In fact, some samples showed a mass increase due to the extra residue that was formed. Hence, mass measurements do not appear to be the most effective way of determining how much ejecta is left over on the samples. Results of this experiment revealed that the solution could eliminate exposed MVC on fiberglass filter paper but that the samples would require a post-digestion rinse to remove residue, if the filter medium was intended to be reused.

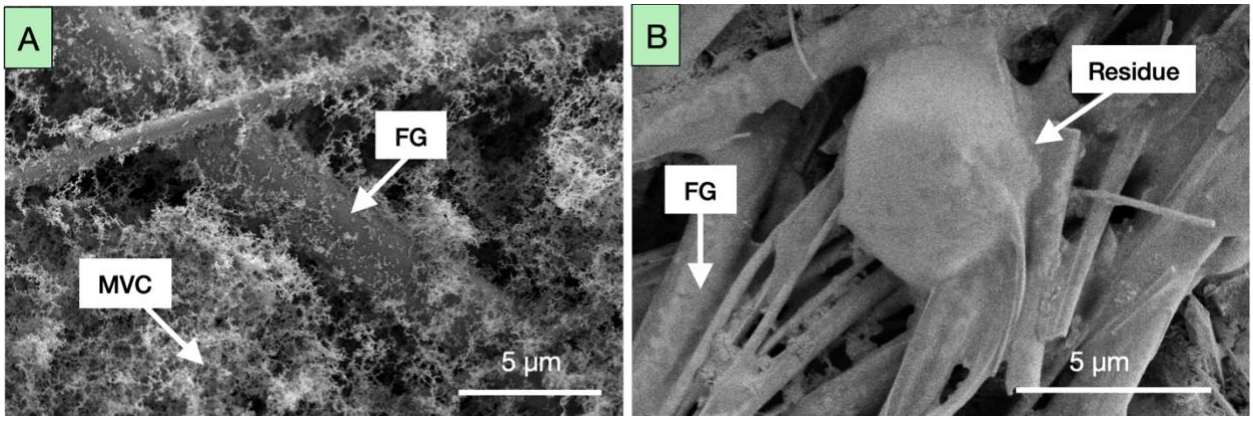

Figure 11. Results from the first preliminary study of digestion. (**A**) SEM images of fiberglass filter paper covered in ejecta from ex-situ collection and then (**B**) after treatment with solutions by Sentecor.

3.3.2 Digestion Study 2

Similar to the first study in Section 3.3.1, the dark sections heavily loaded with condensate and ejecta decreased in color significantly. For the control samples maintained in water (**Fig. 12A**), the ejecta remaining on the filter indicated that the act of soaking and rinsing did not remove ejecta by agitation alone. However, the change in loading was evident for the samples soaked in one of the solvents, even within the first 20 minutes. Furthermore, the solvents appeared to partially strip away the nylon and polyethylene terephthalate (PET) support from the filter paper as seen in **Fig. 12B**.

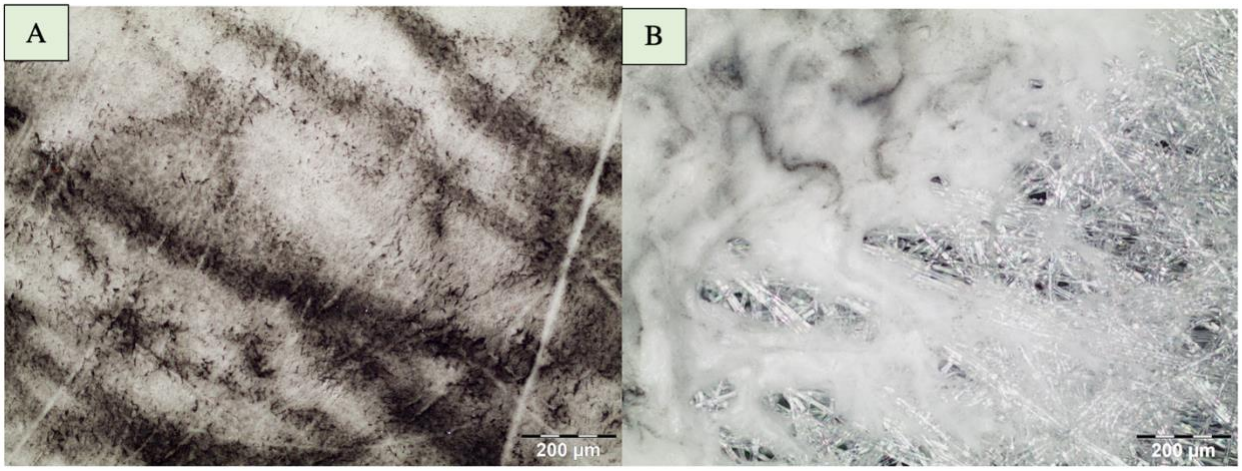

Figure 12. Light Optical Microscopy images of two nylon and ejecta samples after (**A**) soaking in DI water for 24 hours (control), and (**B**) after soaking in Solution 12 for 20 minutes. Treated samples exhibit very little Ti byproducts but show remaining residue.

3.4 Thermal Analysis and Reactivity

3.4.1 Bomb Calorimetry

Bomb calorimetry was expected to provide the most useful information concerning the combustion energy related to reactions involving ejecta and MVC. A series of samples consisting of ethanol as a control material were tested to understand the heat capacity of the bomb. The components of the bomb calorimeter are shown in **Fig. 13A**. The heat capacity of the bomb was added to the tests involving metal particles to compensate for the heat absorbed by the bomb itself. Results for these preliminary tests showed that there were large differences in the heat capacity for the control solution, apparently due to variance caused by the machine. That variance then contributed to the results of the materials being tested. Results for the combustion of pure titanium nano powder are shown in **Table 3** and exhibit a relatively high degree of variance. After combustion, there would be regions of melted metal as well as white powder in the combustion chamber as shown in **Fig. 13B**, which suggested that the combustion reaction

was incomplete. The rather large variation and incomplete reaction that occurred with pure Ti powder was not desirable. It also did not provide confidence for evaluating the irregular material like MVC, since this commercial titanium was assumed to be more consistent.

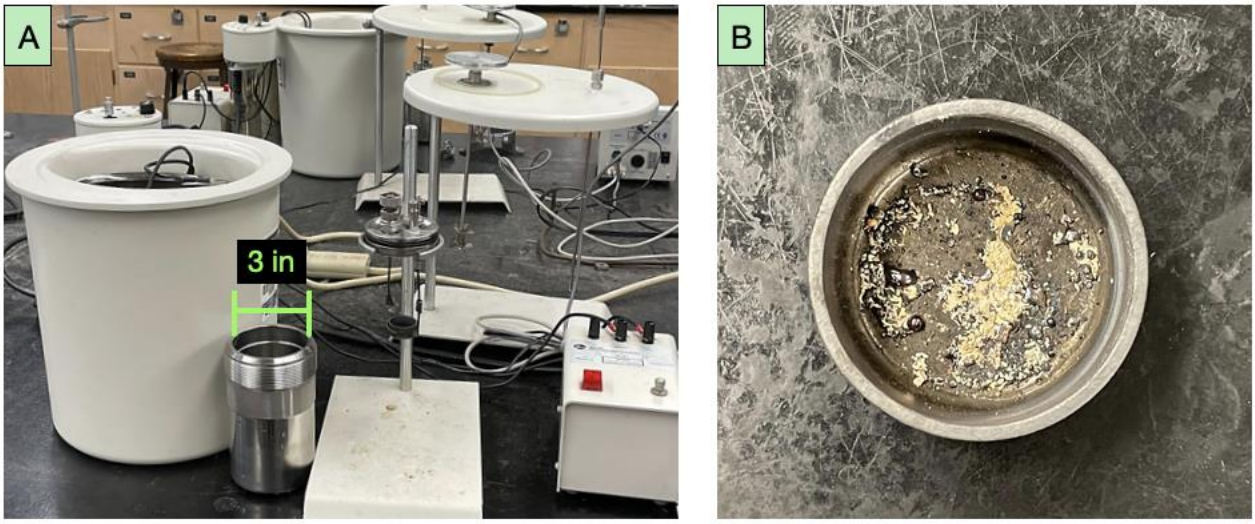

Figure 13. (**A**) A bomb calorimeter with its components separated and the inner diameter of the bomb indicated for scale, (**B**) residue left behind by combusted titanium nano powder.

Table 3. Average heat of reaction from each material placed in the bomb calorimeter.

Material	Avg. Heat of Reaction (cal/C)*	Standard Deviation	COV
Bomb and Ethanol	7610	580	0.076
Titanium Nano Powder	5100	2000	0.392
Ti6Al4V Feedstock Powder	4480	2040	0.456
*Calculated Bomb Heat Capacity: 515 ± 51 (cal/C)			

3.4.2 Thermogravimetric Analysis

The basis of thermogravimetric analysis (TGA) is that a small amount of sample is heated while the weight is monitored, allowing the user to observe reactions that rely on mass change such as oxidation. Here, we applied TGA to evaluate oxidation of the metal samples as

seen in **Fig. 14** for the pure Ti nano-powder. In contrast to the responses from bomb calorimetry, the results from TGA showed consistent mass increase of the titanium nano powder over different ramp rates. A 40% mass increase is estimated when assuming all titanium converts to TiO2 as calculated from the mass ratio in Equation 1. There was no evidence of ignition at an earlier over the heating range regardless of the ramp rates (i.e. from 5 to 12 °C/min).

$$Ti(s) + O_2(g) \rightarrow TiO_2(s) \quad (1)$$

TGA was also performed on the in-situ ejecta on fiberglass filter tabs and the fiberglass tabs without metal loading. A comparison of the fiberglass (FG) material to the in-situ samples with loading is shown in **Fig. 15.** Oxidation of the ejecta can be observed by the mass increase beginning at approximately 700°C. Although the fiberglass behavior contributes noise to the thermal signature as a background signal, a distinct oxidation reaction is evident. The in-situ samples had an estimated 10 wt% of ejecta with the balance being the fiberglass filter tab. Therefore, a 4 wt% increase was expected from the overall sample due to oxidation. Both the ejecta and fiberglass samples (shown in green) in Fig. 15 have comparable weight percent increases, with one sample having a 5 wt% increase as indicated, and the other having a 4% increase. When comparing the in-situ samples that were treated with Sentecor's solutions, there was negligible weight percent increase after 600°C for the samples digested for 2 hours and for 24 hours. This further showed that the post-digested samples had little to no metal left, and so no oxidation reaction occurred. **Fig. 16** compares the oxidation reaction of pure titanium nano powder to the ejecta on fiberglass and the sample soaked in Solution 11 for 2 hours.

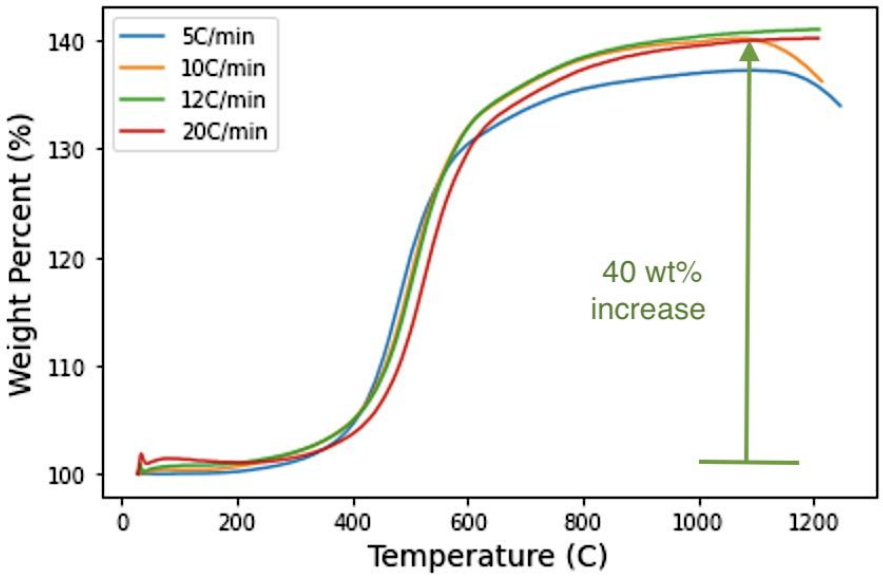

Figure 14. Results from TGA of titanium nano powder using different temperature ramp rates.

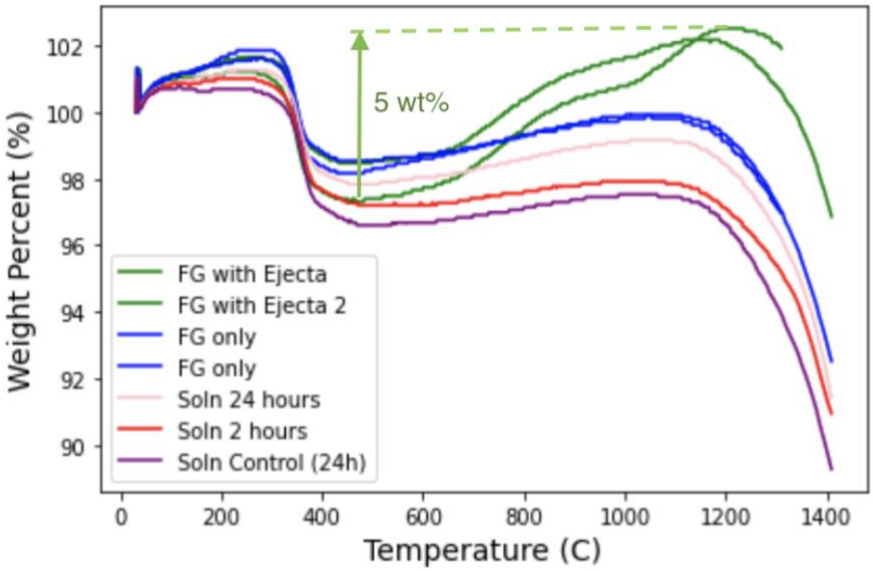

Figure 15. Results for TGA of fiberglass paper tab (FG), FG with ejecta, and FG with ejecta after being digested with Solution 11 by Sentecor, conducted at 12 °C/min.

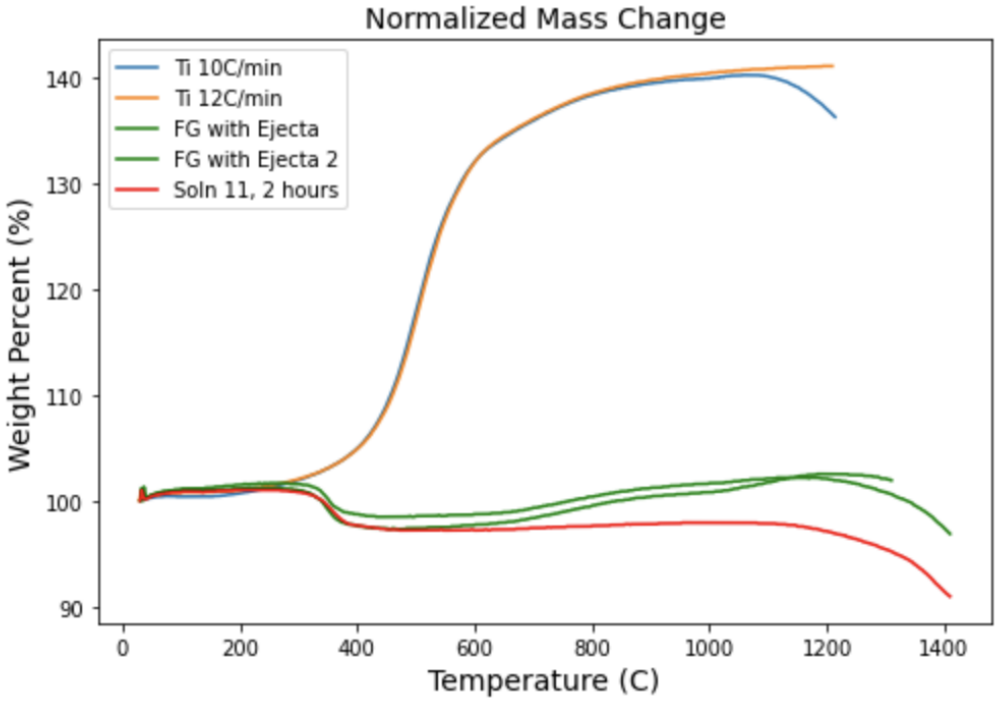

Figure 16. Comparing the mass change of Ti nano powder to the fiberglass samples with ejecta and ejecta samples soaked in Solution 11.

Overall, TGA proved to be a more sensitive method for assessing the thermal response of the ejecta and MVC. The findings also highlighted the importance of the background material thermal characteristics that was used to collect and hold the ejecta. If the filter material changed weight drastically, it would be difficult to isolate the oxidation behavior of ejecta, especially if the background material degraded and lost weight at the same time. Other candidate filter materials were heated with TGA including nylon filter papers and PTFE, but these had notable degradation regions between 400 to 600 °C, which was in the temperature range of the oxidation. Preliminary experiments conducted with Alumina showed that it did not undergo weight changes all the way through 1200°C, making it an ideal background for TGA measurements in the future.

Chapter 4 - Discussion

In response to the first specific aim, various methods were applied to collect MVC from within the build chamber of a standard EOS M 290 SLM machine. Results showed that the in-situ collection consisting of filter tabs placed in the exhaust baffle served as a flexible method that could pick up high concentrations of MVC. Over 1.5 mg of metal was collected on many of the samples over the period of a small build (12 hours), providing dense material in controllable quantities that didn't require sampling of the MVC waste container. Smaller builds could be performed if necessary to collect sufficient quantities of MVC to reduce powder use. Builds longer than 12 hours were not conducted with in-situ collection, and it will be interesting to see if the degree of loading is substantially greater that noted after the 12 hour builds described herein.

The in-situ collection method can be applied to a variety of different substrate materials, such as filter papers, tape and metal foil. Using a diversity of background materials will support multiple types of characterization or improved techniques. For example, using copper foil as a backing can result in higher resolution for EDS and better elemental analysis due to copper being highly conductive and easily removed from the background. In-situ collection is anticipated to be especially useful for conducting reactivity experiments, as the surface of the substrate can be completely coated with ejected material. Alternatively, collecting material ex-situ can be a quick way to obtain material for viewing under a microscope without risking the cost and time of conducting a build.

It is important to characterize the size and morphology of MVC, as metal particles ignite at lower temperatures in the nanoparticle form [20]. Metal nanoparticles are extremely reactive. Single isolated particles were rarely encountered, whereas agglomerates were observed

due to the increasing effect of adhesion forces with decreasing size [26]. The large mats of MVC as shown in Fig. 9B still have a high surface area and expected reactivity. Therefore, a combination of characterization tools for determining the individual nanoparticle sizes as well as the larger agglomerations is necessary. The individual MVC nanoparticles were found to range from 20-40 nm. From the studies reported by Keaveney et al. for Ti6Al4V MVC and Noskov et al. for steel, the nanoparticles were typically around 10-20 nm [7, 12]. The particles observed in this study are very consistent with that range.

According to the elemental composition performed by EDS, the MVC contained 18 wt% Al and 2 wt% V in comparison to the 6 wt% Al and 4 wt% V of Ti6Al4V feedstock powder. The higher Al content is attributed to the difference in vaporization temperatures between these elements, as aluminum is the lighter element and vanadium is heavier. These elemental differences were also observed by Keaveney et al. for MVC produced from Ti6Al4V powder, who found an elemental ratio of 27.5 Al, 69.5 Ti, and 2.4 V (in wt%). Other groups that measured the elemental composition of larger ejected particles like spatter showed that the chemistry remained similar to the feedstock powder [7, 10].

While a combination of passivation methods like silicone oil and quartz sand can be used on MVC to prevent ignition, we went one step further to eliminate MVC altogether. Proprietary solutions created by Sentecor allowed ejecta to be visibly dissolved in a slow and safe manner. The lack of oxidation reaction shown in TGA measurements was further proof that the metal had been eliminated from the filter tabs. It was promising that this reaction could be performed directly on the fiberglass filter papers used in the EOS M 290 filtration system. That approach should be advanced to further evaluate the potential for digesting waste byproducts generated during laser powder bed fusion.

To understand the reactivity of MVC, a survey of many different thermal techniques was conducted. There were limitations to this effort, including what instruments were available at the UW or within reasonable distance, as well as the minimal quantity of MVC needed for those techniques. For instance, bomb calorimetry required samples near 1 g, and the instrument was not found capable of measuring heat of combustion as accurately as desired. In comparison, TGA proved to be much more reliable than bomb calorimetry in assessing thermal behavior and required smaller sample sizes < 1 mg of powder. The results were highly repeatable. However, there was no evidence of ignition occurring in measurements performed with pure titanium nanoparticles, even with higher temperature ramp rates. An ignition reaction would be seen by a sharp increase in mass rather than a gradual increase as observed in Fig. 14 [22, 23]. The ideal measurement of MVC reactivity would include ignition. Regardless, TGA remains a characterization option for accurately measuring the oxidation behavior of ejecta produced from SLM. Future work should explore techniques for evaluating flash/ignition temperature of the MVC.

Chapter 5 – Conclusions and Future Work

5.1 Conclusions

One of the most overlooked concerns in powder bed fusion by SLM is the byproducts that are generated. Metal vapor condensate (MVC), in particular, poses a risk of ignition and is difficult to dispose of in a safe manner. It poses a hazard to operators as well as the environment and contributes substantial additional cost to this approach to manufacturing. This project was

focused on the collection, characterization, and reactivity assessment of ejecta material generated in during builds performed with EOS M290 machine and Ti6Al4V feedstock.

Two forms of collection were pursued in this study, which both focused on the baffle for the exiting argon gas within the printing chamber. The first method was an ex-situ collection method that involved swabbing or rinsing the baffle after a print occurred. This collected small amounts of ejected material that could be viewed under SEM and assessed for particle size analysis and chemical composition. However, the mass of metal material was too low for reactivity experiments, so a second method of in-situ collection was tested. The second approach, i.e. in-situ collection, involved inserting a set of filter tabs onto the baffle to pick up ejecta during a print. The in-situ approach resulted in over 1.5 mg of ejecta collected on some samples. In addition, facing the sample tabs away from the build plate allowed the surface to be shielded from the direct stream of spatter and increased the amount of MVC collected.

The collected MVC consisted of 20-40 nm particles agglomerated into mass networks and would stick to all surfaces of ejected particles or spatter. The elemental composition of MVC was also distinctly different from spatter or feedstock Ti6Al4V powder. Consistent with a previous report, the MVC had a higher concentration of aluminum. While spatter contained approximately 4.3 wt% aluminum, which is closed to that of the virgin powder feedstock, the MVC had 18.3 wt%.

Studies aimed at digesting ejecta were conducted with the help of Sentecor Solutions using an environmentally benign solution of proprietary composition. Visually, we observed that after being in solution for 4 hours the ejecta collected ex-situ on both fiberglass and nylon fiber paper could be completely eliminated. TGA analysis was used to confirm that there was no oxidation reaction occurring in the filter paper samples after the digestion. Measuring the weight

of samples before and after treatment was not a reliable way of determining how much ejecta was removed as a result of excess residue coating the samples.

Finally, a preliminary effort was performed to characterize the reactivity of small samples of metal nanoparticles using TGA. The effectiveness of passivation methods to resist combustion that are applied to MVC could also be compared. TGA was found to be a reliable measurement of oxidation, however, there was no indication of ignition occurring when experimenting with titanium nanoparticles. Future work is required on this topic.

5.2 Future Work

The next stages of this project involve assessing the effectiveness of different passivation methods to reduce the potential for ignition of MVC. Undoubtedly, this topic would be of substantial value to industry and could have a substantial impact on the literature in this area. We plan to test the thermal behavior of a wide range of passivation methods, such as different oils with sand, calcium carbonate or chalk. These are the existing approaches used to passivate MVC While it would be helpful to obtain the data on ignition such as through bomb calorimetry, it may be difficult to find an instrument with adequate sensitivity and capable of evaluating the combustion response with less than a milligram of material.

As an alternative to bomb calorimetry, TGA could serve as an acceptable alternative. A preliminary evaluation of passivation materials was conducted using TGA. A comparison of different materials used as background collection materials as well as in the passivation process is shown in **Fig. 17**. This comparison includes the alumina collection tab, sand, dehydrated sand and fiberglass. These early results show that the base materials would likely not conflict with the metal response and its capacity for oxidation could be evaluated using TGA. Hence, this process

could support a more thorough investigation of the behavior of ejecta under different passivation conditions.

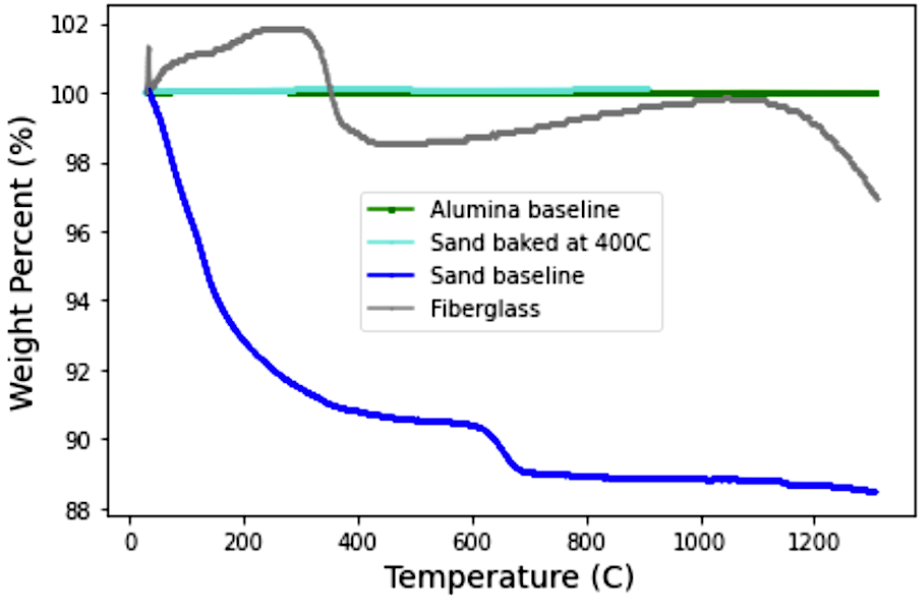

Figure 17. TGA data for potential baseline materials, at a ramp rate of 12 C/min.

References

1. B. Blakey-Milner, P. Gradl, G. Snedden, M. Brooks, J. Pitot, E. Lopez, M. Leary, F. Berto, A. Plessis, "Metal Additive Manufacturing in Aerospace, a Review," *Materials and Design*, vol. 209, 2021, doi: 10.1016/j.matdes.2021.110008.

2. W. E. King, A. T. Anderson, R. M. Ferencz, N. E. Hodge, C. Kamath, S. A. Khairallah, A. M. Rubenchik, "Laser powder bed fusion additive manufacturing of metals; physics, computational, and materials challenges," *Appl. Phys. Rev.*, vol. 2, no. 4, 2015, doi: 10.1063/1.4937809.

3. E. Santecchia, S. Spigarelli, M. Cabibbo, "Material Reuse in Laser Powder Bed Fusion: Side Effects of the Laser-Metal Powder Interaction," *Metals*, vol. 10, no. 3, 2020, doi: 10.3390/met10030341.

4. X. Wang, Z. Wang, L. Ni, M. Zhu, C. Liu "Explosion characteristics of aluminum powder in different mixed gas environments," *Powder Technology*, vol. 369, pp. 53-71, 2020, doi: 10.1016/j.powtec.2020.04.056.

5. A. Ladewig, G. Schlick, M. Fisser, V. Schulze, U. Glatzel," Influence of the shielding gas flow on the removal of process by-products in the selective laser melting process," *Addit. Manuf.*, vol. 10, pp. 1-9, 2016, doi: 10.1016/j.addma.2016.01.004.

6. A. Sutton, C. Kriewall, M. Leu, "Characterization of Heat-Affected Powder Generated During the Selective Laser Melting of 304L Stainless Steel Powder," *2017 International Solid Freeform Fabrication,* 2017.

7. S. Keaveney, A. Shmeliov, V. Nicolosi, D. P. Dowling, "Investigation of process by-products during the Selective Laser melting of Ti6Al4V powder," *Additive Manufacturing*, vol. 36, 2020, doi: 10.1016/j.addma.2020.101514.

8. Herding Filtration systems, *Safe Filtration in Additive Manufacturing*, Herding GmbH Filtertechnik.

9. A. Montelione, S. Ghods, R. Schur, C. Wisdom, D. Arola, M. Ramulu, "Powder Reuse in Electron Beam Melting Additive Manufacturing of Ti6Al4V: Particle Microstructure, Oxygen Content, and Mechanical Properties," *Additive Manufacturing*, vol. 35, 2020, doi: 10.1016/j.addma.2020.101216.

10. J. Achinadka. "Study of Condensate generated during Direct Metal Laser Sintering," *Proceedings of the ASME 2017 Gas Turbine India Conference,* 2017.

11. M. Sousa, P. Arezes, F. Silva, "Nanomaterials exposure as an occupational risk in metal aditive manufacturing," *J. Phys.: Conf.*, vol. 1323, no. 6, 2019, doi: 10.1088/1742-6596/1323/1/012013.

12. A. Noskov, T. K. Ervik, I. Tsivilskiy, A. Gilmutdinov, Y. Thomassen, "Characterization of ultrafine particles emitted during laser-based additive manufacturing of metal parts," *Sci. Rep.*, vol. 10, 2020, doi: 10.1038/s41598-020-78073-z.

13. A. Jensen, H. Harboe, A. Brostrøm, K. A. Jensen, A.S. Fonseca. Nanoparticle Exposure and Workplace Measurements During Processes Related to 3D Printing of a Metal Object. *Front. Public Health*, 2020, doi: 10.3389/fpubh.2020.608718.

14. P. Graff, B. Ståhlbom, E. Nordenberg, A. Graichen, P. Johansson, H. Karlsson, "Evaluating Measuring Techniques for Occupational Exposure during Additive Manufacturing of Metals: A Pilot Study," *Journal of Industrial Ecology*, vol. 21, no. S1, pp. S120-S129, 2016, doi: 10.1111/jiec.12498.

15. R. A. Yetter, G. A. Risha, S. F. Son, "Metal particle combustion and nanotechnology," *Proceedings of the Combustion Institute*, vol. 32, no. 2, pp. 1819-1838, 2009, doi: 10.1016/j.proci.2008.08.013.

16. Sintavia, "Overview of Disposal Procedures for Powder Condensate within Metal Powder Bed Fusion," *Sintavia, LLC,* 2021.

17. R. J. Jacob, Boran Wei, Michael R. Zachariah, "Quantifying the enhanced combustion characteristics of electrospray assembled aluminum mesoparticles," *Combustion and Flame,* vol. 167, pp. 472-480, 2016, doi: 10.1016/j.combustflame.2015.09.032.

18. C. Kong, Q. Yao, D. Yu, S. Li, "Combustion characteristics of well-dispersed aluminum nanoparticle streams in post-flame environment," *Proceedings of the Combustion Institute,* vol. 35, no. 2, pp. 2479-2486, 2015, doi: 10.1016/j.proci.2014.06.127.

19. P. T. Lynch, "High Temperature Spectroscopic Measurements of Aluminum Combustion in a Heterogeneous Shock Tube," *University of Illinois*, Department of Mechanical Sci. and Engineering, 2010.

20. V. Zarko, A. Glazunov, "Review of Experimental Methods for Measuring the Ignition and Combustion Characteristics of Metal Nanoparticles," *Nanomaterials (Basel),* vol. 10, 2020, doi: 10.3390/nano10102008.

21. Q. Tran, I. Altman, P. Dube, M. Malkoun, R. Sadangi, R. Koch, M. L. Pantoya, "Direct demonstration of complete combustion of gas-suspended powder metal fuel using bomb calorimetry," *Meas. Sci. Technol.*, vol. 33, no. 4, 2022, doi: 10.1088/1361-6501/ac47bc.

22. F. Noor, H. Zhang, T. Korakianitisac, D. Wen, Phys, "Oxidation and Ignition of Aluminum Nanomaterials," *Phys. Chem. Chem. Phys.*, vol. 15, no. 46, pp. 20176-20188, 2013, doi: 10.1039/C3CP53171F.

23. D. E. G. Jones, R. Turcotte, R. C. Fouchard, Q. S. M. Kwok, A. Turcotte, Z. Abdel-Qader, "Hazard Characterization of Aluminum Nanopowder Compositions," *Propellants, Explosives, Pyrotechnics*, vol. 28, no. 3, pp. 120-131, 2003, doi: 10.1002/prep.200390018.

24. C. E. Johnson, S. Fallis, A. P. Chafin, T. J. Groshens, K. T. Higa, “Characterization of Nanometer- to Micron-Sized Aluminum Powders: Size Distribution from Thermogravimetric Analysis,” *Journal of Propulsion and Power*, vol. 23, no. 4, pp 669-682, 2007, doi: 10.2514/1.25517.

25. D. Laboureur, G. Glabeke, J. B. Gouriet, “Aluminum nanoparticles oxidation by TGA/DSC,” *J. Therm. Anal. Calorim.*, vol. 137, pp. 1199–1210, 2019, doi: 10.1007/s10973-019-08058-2.

26. A. Gromov, U. Teipel, in *Metal Nanopowders*, Wiley-VCH, Weinheim, Germany 2014, Ch. 5.

Appendix A.

EOS Ti6Al4V Feedstock Powder Properties from Certificate of Inspection

Analyses of Powder (see page 4 for analysis details)

Sampling and Analysis Sample Preparation

Sampling of the quality assurance test batch and analysis sample preparation done according to ASTM B215.

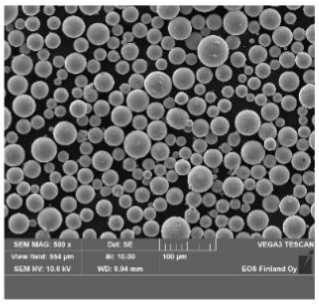

Cleanliness of Powder

Powder is visually free from foreign materials and uniform in condition.

Morphology

Powder is predominantly spherical with low levels of deformed particles.

Particle Size Distribution Analysis

Test method	Size characteristic	Limits	Result	✓/✗	Test Method	Size charateristic	Result
Laser diffraction	d10 **[µm]**	**22 - 32**	30	✓	Dynamic image analysis x_{Cmin}	x10 **[µm]**	24
	d50 **[µm]**	**34 - 44**	41	✓		x50 **[µm]**	37
	d90 **[µm]**	**49 - 61**	57	✓		x90 **[µm]**	50

Sieve Analysis

Fraction retained	Test Method	Limits	Result	✓/✗
≥ 63 µm **[wt%]**	Laboratory sieving	**Max. 0.5**	0.0	✓

Powder Density Analysis

Property	Test Method	Limits	Result	✓/✗
Apparent density **[g/cm³]**	ASTM B212	**2.40 - 2.80**	2.59	✓
Skeletal density **[g/cm³]**	Gas displacement	**N/A**	4.416	N/A

Powder Water Content Analysis

Property	Test Method	Limits	Result	✓/✗
Water content **[ppm]**	Coulometric KF titration	**Max. 125**	40	✓

Chemistry Analysis (External ISO 17025 accredited laboratory)

Element	Test Method	Limits [wt.%]	Result	✓/✗	Element	Test Method	Limits [wt.%]	Result	✓/✗
Ti	ICP-OES	**Balance**	Bal.	✓	N	Fusion	**Max. 0.04**	0.02	✓
Al	ICP-OES	**5.50 - 6.75**	6.32	✓	H	Fusion	**Max. 0.012**	0.002	✓
V	ICP-OES	**3.50 - 4.50**	4.02	✓	Y	ICP-OES	**Max. 0.005**	<0.001	✓
Fe	ICP-OES	**Max. 0.25**	0.21	✓	OE, each	ICP-OES	**Max. 0.10**	<0.10	✓
O	Fusion	**Max. 0.15**	0.15	✓	OE, total	ICP-OES	**Max. 0.40**	<0.40	✓
C	Combustion	**Max. 0.08**	0.01	✓					